Hypertension Research (2018) 41:578–588
https://doi.org/10.1038/s41440-018-0061-1

ARTICLE

Gitelman's Syndrome: characterization of a novel c.1181G>A point mutation and functional classification of the known mutations

Verdiana Ravarotto[1,2] · Johannes Loffing[3] · Dominique Loffing-Cueni[3] · Michèle Heidemeyer[3] · Elisa Pagnin[2] · Lorenzo A. Calò[2] · Gian Paolo Rossi[1]

Received: 25 September 2017 / Revised: 22 December 2017 / Accepted: 29 December 2017 / Published online: 20 June 2018

Abstract

We have investigated the mechanisms by which a novel missense point mutation (c.1181G>A) found in two sisters causes Gitelman's syndrome by impairing the sodium chloride co-transporter (NCC, encoded by SLC12A3 gene) function. The cDNA and in vitro transcribed mRNA of either wild-type or mutated SLC12A3 were transfected into HEK293 cells and injected into Xenopus laevis oocytes, respectively. The expression, maturation, trafficking, and function of the mutated and wild-type NCC were assessed by Western blotting, immunohistochemistry and $^{22}Na^{+}$ uptake studies. By immunoblotting of lysates from HEK293 cells and oocytes expressing wild-type NCC, two NCC-related bands of approximately 130 kDa and 115 kDa, corresponding to fully and core-glycosylated NCC, respectively, were identified. In contrast, the mutant NCC only showed a single band of approximately 115 kDa, indicating impaired maturation of the protein. Moreover, oocytes injected with wild-type NCC showed thiazide-sensitive $^{22}Na^{+}$ uptake, which was absent in those injected with the mutant NCC. The novel mutation was discussed in the context of the functionally characterized NCC mutations causing Gitelman's syndrome, which fit into five classes. In conclusion, the functional characterization of this novel Gly394Asp NCC and its localization on the NCC structure, alongside that of previously known mutations causing Gitelman's syndrome, may provide novel information on the function of the different domains of the human NCC.

Introduction

Gitelman's syndrome (GS, OMIM no. 263800) is an inherited autosomal recessive disease caused by loss-of-function mutations in the sodium-chloride co-transporter (NCC) in the renal distal convoluted tubule (DCT). After its description in 1966, its estimated prevalence (1:40.000) was found to be higher than initially held. Moreover, heterozygous carriers were found to be present in approximately 1% of the Caucasian population, thus making GS one of the most frequently inherited renal tubular disorders [1]. Clinically, GS presents in adolescence or early adulthood with muscle weakness, fatigue, joint pain, cramps, tetany, reduced peripheral resistance, normal or low blood pressure and resistance to the pressor effect of vasoconstrictors, such as angiotensin II and norepinephrine, with consequent marked activation of the renin-angiotensin-aldosterone system (RAAS) [2–4]. Its biochemical hallmarks comprise hypokalemia, metabolic alkalosis, sodium wasting, hypomagnesemia, hypocalciuria, and secondary aldosteronism [1].

Loss-of-function mutations of the solute carrier family 12 member 3 gene SLC12A3 coding for NCC in the DCT, resulting in renal sodium wasting, underlie the molecular changes. The sodium loss triggers adaptive responses in the kidney, including activation of the renin synthesis and aldosterone-driven excretion of K^{+} in exchange for Na^{+} [5].

A screening of 2492 members of the Framingham Heart Study (FHS) for variation in three genes causing Gitelman's and the related Bartter's syndrome allowed the detection of 138 variants in the coding sequence [6]. A proportion of them were associated with significantly lower age-adjusted and sex-

Electronic supplementary material The online version of this article (https://doi.org/10.1038/s41440-018-0061-1) contains supplementary material, which is available to authorized users.

✉ Gian Paolo Rossi
gianpaolo.rossi@unipd.it

[1] Internal Medicine, Department of Medicine–DIMED, University of Padova, Padova, Italy

[2] Nephrology, Department of Medicine–DIMED, University of Padova, Padova, Italy

[3] Institute of Anatomy, University of Zurich, Zurich, Switzerland

adjusted systolic and diastolic blood pressure (BP) leading to the contention that they can blunt the hypertension phenotype in hypertensive patients. While suggesting that alleles altering renal sodium handling affect BP in the general population, these results indicated that the prevalence of GS mutations may have been grossly underestimated, inasmuch as GS is usually suspected only in patients with hypotension, rather than in those with normal BP or high BP.

The cloning and characterization of the SLC12A3 gene encoding NCC led to the discovery of more than 300 mutations (HGMD database: www.hgmd.cf.ac.uk), including missense, nonsense, frame-shift, and splice site mutations, which result in dysfunction of the cotransporter [7]. Notwithstanding this large number, the underlying molecular mechanisms remain poorly understood because only approximately 44 mutations have been functionally characterized. Thus far, the putative mechanisms include reduced NCC synthesis, blunted NCC activation, enhanced NCC degradation, and impaired NCC trafficking to the cell surface [8].

We recently discovered a novel NCC point mutation (c.1181G>A ref. NM_000339.2 following HGVS nomenclature) in two young sisters, one of whom showed the full-blown syndrome and the other had a milder clinical phenotype. This mutation causes a Gly394Asp amino acid substitution at a site close to the seventh extracellular loop. This mutation was not present in the GS registry established at the University of Padua over 30 years ago and in public databases. Hence, we thought it interesting to characterize this mutation using a combined molecular and functional approach.

Methods

Synthesis of wt-NCC and G394D-NCC cRNA

cDNA of human wild-type (wt-NCC) and mutated NCC (G394D-NCC) (GeneCopoeia, Rockville, MD, USA) were cloned in pSDeasy vector. After linearization of the plasmid with *PciI* (New England Biolabs, Ipswich, MA, USA), cRNA synthesis was performed using the MEGAScript SP6 kit (Ambion, Carlsbad, CA, USA) according to the manufacturer's instructions. cRNA was purified (Nucleospin RNA; MacheryNagel, Oensingen, CH) and the integrity of the transcription product was confirmed by agarose gel electrophoresis.

In vitro experiments

The human embryonic kidney cell line HEK293 (American Type Cell Culture, ATCC, Manassas, VA, USA), was cultured in Eagle's Minimum Essential Medium supplemented with 10% fetal bovine serum (FBS) (Sigma Aldrich, Saint Louis, MO, USA). After the second passage, cells were plated in 6-well plates and transfected with coding sequences for NCCwt, NCCmut and green fluorescent protein (GFP). After replication of expression vectors ORF cDNA clones (GeneCopoeia, Rockville, MD, USA) in bacteria, wt-NCC, G394D-NCC, and GFP DNAs were transfected into the cells by lipofection using Metafectene® (Biontex Laboratories GmbH, München, DE). After protocol optimization, cells were selected 24 and 48 h after transfection.

cRNA injection in X. laevis oocytes

X. laevis oocytes at stage IV–V were injected with 0.05 µl cRNA (44 µg/µl) of wt-NCC and G394D-NCC or with 0.05 µl H_2O as a control. Oocytes were incubated at 16 °C for 72 h in modified Barth's Solution (88 mM NaCl, 1 mM KCl, 0.41 mM $CaCl_2$, 0.82 mM $MgCl_2$, 0.33 mM $Ca(NO_3)_2$, 2.4 mM $NaHCO_3$, 10 mM HEPES/Tris, pH 7.4) with gentamicin (5 mg/l) and doxycyclin for translation of the protein. The solutions were changed daily. After 72 h, the oocytes were processed to analyze the expression, trafficking and activity of NCC by Western blot, immunohistochemistry and $^{22}Na^{+}$-uptake experimentation, respectively.

Immunoblotting

To evaluate NCC protein expression, we extracted proteins from the cells transfected using a lysis buffer (150 mM NaCl, 50 mM Tris-HCl pH 8.00, 1% Triton-X-100, Protease and Phosphatase Inhibitors, Roche, BS, CH). To detect NCC in oocytes, 3 to 10 oocytes per group were pooled and lysed in 30 to 100 µl lysis buffer. To quantify proteins, a Bradford assay with protein standards was performed (CooAssay Protein Dosage Reagent, Uptima, FR). Protein samples from HEK293 cells and an equivalent of one oocyte per lane were separated by 8% polyacrylamide gel electrophoresis. After electrophoretic separation, proteins were transferred to nitrocellulose membranes, which were then blocked for 30 min in blocking buffer (Odyssey blocking buffer, Li-Cor Biosciences, Lincoln, NE, USA) and incubated with primary antibodies against N-terminal tail of NCC (Millipore, Burlington, MA, USA) diluted 1:4000 at 4 °C overnight. The membranes were further incubated for 2 h with goat anti-rabbit IRD800 antibody (1:20000; LI-COR, Bad Homburg, DE) diluted 1:10000 and visualized with Odyssey imager (Li-Cor Biosciences, Lincoln, NE, USA). A monoclonal antibody against α-tubulin diluted 1:10000 was used for normalization of HEK293 immunoblotting. Loading of an equal amount of protein in the oocyte experiments was verified by immunodetection of GAPDH with a mouse monoclonal antibody (1:4000; Ambion, Carlsbad, CA, USA).

Immunofluorescence in HEK293 cell line

To detect whether the cells acquired the plasmids, the cells were grown on glass coverslips, transfected with wt-NCC, G394D-NCC and GFP DNAs, and fixed at 4 °C with the fixation solution (PFA 3%, PBS pH 7.3). After overnight fixation and washing three times with PBS, the cells were pre-incubated with PBS/BSA 2% for 10 min, followed by incubation with 0.5% Triton-100, washing steps, and incubation with an anti-N-terminal tail of NCC antibody diluted 1:2000 at 4 °C overnight. The following day, coverslips were rinsed and incubated for 2 h in the dark with a secondary CY3-labeled goat anti-rabbit antibody diluted 1:1000 (Jackson Immuno Research, West Grove, PA, USA) and DAPI diluted 1:1000 and PBS/BSA 2% for nuclei staining. After washing, the glycerol mounting medium with DABCO was added and incubated for 2 h at 4 °C. Images were examined with a confocal Leica microscope. Images were acquired with a CCD camera and processed using Adobe Photoshop and Microsoft Power Point software.

Immunofluorescence in oocytes

For immunofluorescence studies, oocytes were fixed with 3% PFA in 0.1 M phosphate buffer (pH 7.3; 300 mOsm) for 4 h at 4 °C and rinsed in phosphate buffer for an additional 2 h. Thereafter, oocytes were frozen in liquid propane, stored at −80 °C, and then processed for immunofluorescence as previously described [9]. In brief, frozen oocytes were cut in 5-µm-thick sections in a cryostat. Unspecific binding sites were blocked with 10% normal goat serum and 1% bovine serum albumin in PBS. Cryosections were incubated at 4 °C overnight with an antibody against the N-terminal tail of NCC (1:2000; Millipore, Burlington, MA, USA). Binding sites of the first antibody were detected using a CY3-labeled goat-anti-rabbit antibody (1:1000; Jackson Immuno Research, West Grove, PA, USA). The cell surface of the oocytes was labeled by detecting the microvillus actin cytoskeleton with Fluorescein Phalloidine (1:50; Biotium, Hayward, CA, USA). After repeated washing, sections were cover-slipped and examined with a fluorescence microscope (Leica DM6000 B, Leica Microsystems, Wetzlar, DE). Images were acquired with a CCD camera and processed by Adobe Photoshop and Microsoft Power Point software.

$^{22}Na^{+}$-uptake experiments

For $^{22}Na^{+}$-uptake experiments, we followed the protocol of Monroy et al. [10]. Seventy-two hours after infection, oocytes were washed and incubated for 30 min at 30 °C in isotonic K^{+}- and Cl^{-}-free medium (96 mM Na^{+}-gluconate, 6 mM Ca^{2+}-gluconate, 1 mM Mg^{2+}-gluconate, 5 mM HEPES/Tris (pH 7.4), 1 mM ouabain, 100 µM bumetanide, 100 µM amiloride). Uptake was performed at 30 °C for 60 min in an isotonic K^{+}-free medium (96 mM NaCl, 1.8 mM $CaCl_2$, 1 mM $MgCl_2$, 5 mM HEPES (pH 7.4), 1 mM ouabain, 100 µM bumetanide, 100 µM amiloride) supplemented with 2 µCi/ml $^{22}Na^{+}$ (Perking Elmer, Waltham, MA, USA). To determine thiazide-dependent sodium-uptake, the experiment was performed in the presence or absence of a thiazide-like diuretic (100 µM metolazone in DMSO; Sigma-Aldrich, Saint Louis, MO, USA). $^{22}Na^{+}$ uptake was terminated by washing the oocytes six times in ice-cold K^{+}-free medium to remove extracellular $^{22}Na^{+}$. Oocytes were individually lysed in 10% SDS. Radioactive tracer was detected in a liquid scintillation analyzer (Packard TRI-CARB 2000/2200CA; Perkin Elmer, Boston, MA, USA).

The results of three separate experiments were pooled wt-NCC (No Thiazide = 44; Thiazide = 46), G394D-NCC (No Thiazide = 44; Thiazide = 42), and H_2O (No Thiazide = 43; Thiazide = 44).

Power calculation and statistical analysis

Sample size was preliminarily estimated by using ImageJ software, then analyzed with GraphPad Prism 5. A two-way analysis of variance (ANOVA) was used to assess both the differences between NCC wt and NCC mut glycosylation and the $^{22}Na^{+}$ uptake in the oocytes.

Results

Case description

The index case is a 26-year-old white Caucasian woman who presented with hypokalemia (2.2 mmol/L), metabolic alkalosis (pH 7.49, bicarbonate 36 mmol/L), elevated plasma renin activity (9 ng Ang I/ml/h n.v. 0.65–2.65) and aldosterone concentrations (25.23 ng/dl; n.v. < 12 ng/dl) with normal/low BP (105/75 mmHg), hypocalciuria (1.9 mmol/day; n.v. 2.5–7.5), hypomagnesemia (0.55 mmol/L; n.v. 0.65–1.05), muscular weakness, and fatigue. The patient is currently treated with potassium supplementation (mixture of potassium succinate 1.03 mEq, malate 0.95 mEq, citrate 2.45 mEq, tartrate 0.44 mEq and bicarbonate 4.93 mEq, for a total of 10 mEq) 6 times per day and magnesium (magnesium pidolate 2.25 g, corresponding to 185 mg of Mg^{2+} ion) 5 times per day. The proband's sister (32 years old) was found to carry the same heterozygous mutations but presented with a milder clinical manifestation and a lower need for K^{+} and Mg^{2+} supplementation. Unfortunately, the proband's parent's clinical and genetic evaluation is not available. The pedigree is shown in Fig. 1a.

By analyzing the 26 exons of the SLC12A3 gene of the index case and sister, we found two mutations: c.1925G>A

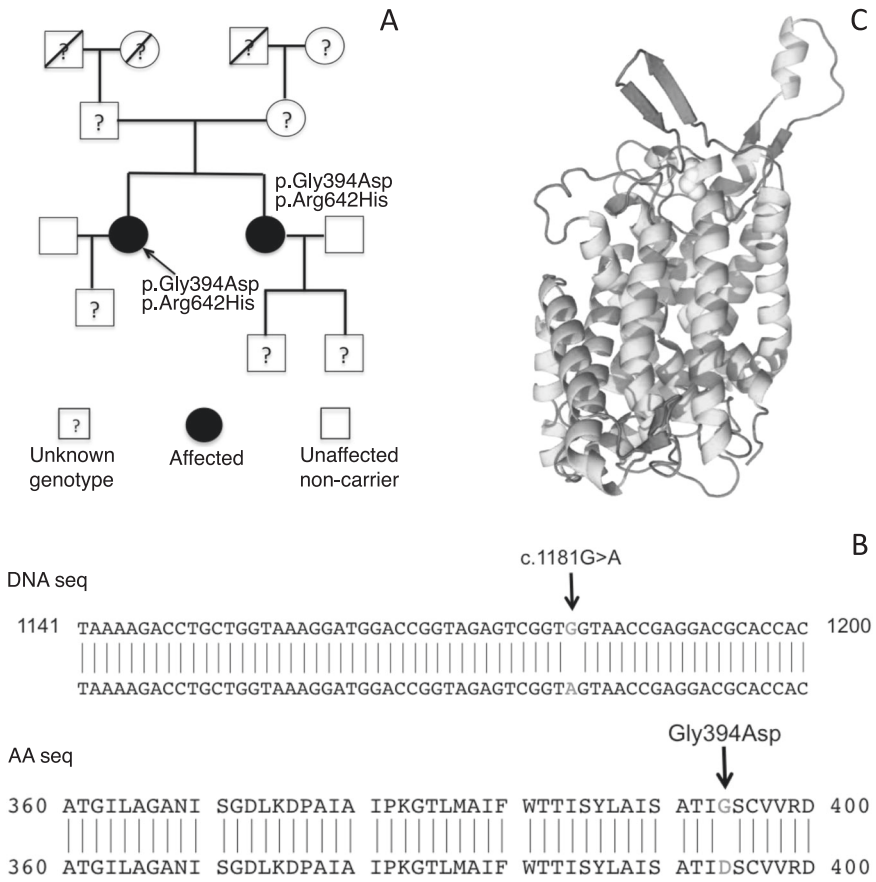

Fig. 1 **a** Genetic pedigree of the proband indicated by the arrow. The parents have not been tested, but the two sisters present the same mutation and are clinically affected by the syndrome. The proband gave birth to a baby boy not yet characterized. **b** Alignment of the wild-type and mutant nucleotide and amino acid sequences. **c** Three-dimensional image of the sodium-chloride co-transporter NCC. Highlighted in yellow is the point mutation G394D in the seventh trans-membrane portion, near the extracellular loop

(Arg642His) and c.1181G>A (Gly394Asp). While the former is one of the most common variants described for the Gitelman's syndrome, the latter has never been described. This finding is consistent with the notion that GS subjects are often compound heterozygous, carrying two different mutations affecting two alleles of an autosome [3, 11]. Since not all the described variants are held to play a functional role in GS, the specific impact of each mutation in the phenotype needed to be clarified. Therefore, we investigated the significance of this mutation for the clinical outcome first using an in silico analysis to predict the impact of a mutation on the protein activity. This preliminary analysis showed that the novel mutation should have a stronger impact compared to the other mutation present (PROVEAN score was −5.71 for G394D vs −4.83 for R642H; http://provean.jcvi.org/index.php). Analysis of the conformation of NCC revealed that the G394D mutation was located near the extracellular loop containing two glycosylation sites in positions 404 and 424 (Fig. 1b, c), while the R642H was much farther off. Figure 2 shows the structure of NCC with all GS mutations that have been functionally characterized thus far, along with the class they belong to.

Transfection of HEK293 cells

Cells were transfected at greater than 70% confluence. We used GFP-transfection and fluorescence microscopy to verify the plasmid insertion in the cells. Transfection with wt-NCC or G394D-NCC plasmids was verified by immunofluorescence using an antibody against NCC [Supplemental Fig. 1].

NCC glycosylation in wild-type and mutant HEK293 cells

To investigate whether the novel mutation affected protein glycosylation, we immunoblotted the wt-NCC and G394D-NCC samples. This evidenced clear-cut differences in protein glycosylation: the wt-NCC showed a band of approximately 130 kDa weight (Fig. 3a), while the mutant G394D-NCC did not (Fig. 3b). Quantification of the glycosylation bands demonstrated a difference between wt-NCC and G394D-NCC at 24 h ($p < 0.003$ 0.233 ± 0.046 vs 0.0268 ± 0.008) and an even more prominent difference at 48 h after transfection ($p < 0.0003$ $0{,}524 \pm 0.084$ vs 0.059 ± 0.012) (Fig. 3c).

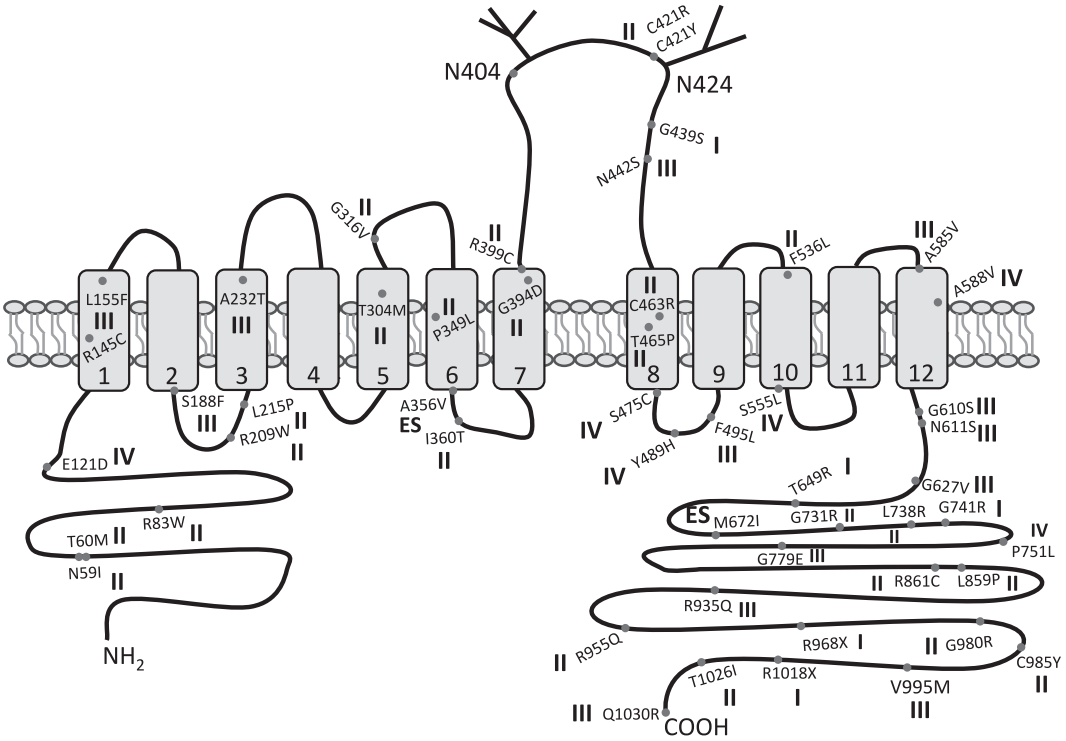

Fig. 2 Topological representation of the Na-Cl cotransporter. Dots highlight the function of mutations described in the literature. Each dot points to a specific mutation, which is described alongside its classification

Impaired glycosylation in G394D-NCC Xenopus laevis oocytes

The Xenopus laevis oocytes lysate was used to detect NCC protein expression in immunoblotting experiments. Injection of wt-NCC plasmid showed after 24 and 48 h a band at approximately 130 kDa, while G394D-NCC only showed the smaller band. The larger glycosylation band was more prominent 48 h after injection (Fig. 4a).

Impaired trafficking and activity of G394D-NCC in Xenopus laevis oocytes

The immunostaining for NCC in Xenopus laevis oocytes showed different staining pattern in the wt-NCC-injected cells, where the protein was detected on the cell surface, and the G394D-NCC-injected cells, in which only intracellular staining was observed. Labeling of the plasma membrane microvillus actin-cytoskeleton with FITC-conjugated phalloidin showed colocalization of the wt-NCC on the cell surface and the G394D-NCC under the cell surface (Fig. 4b).

$^{22}Na^{+}$ uptake

In vehicle-injected oocytes, only a low uptake of $^{22}Na^{+}$ was observed, which fell to 35% after thiazide challenge ($p < 0.05$). In wt-NCC-injected oocytes, the $^{22}Na^{+}$ uptake was increased more than 3-fold (342% higher), indicating that the transfection resulted in functional insertion of the NCC protein in the plasma membrane. Exposure to thiazides blunted $^{22}Na^{+}$ uptake (from 342 to 63%, $p < 0.0001$). By contrast, in the G394D-NCC-injected oocytes, no $^{22}Na^{+}$ uptake was detected in the absence or presence of thiazides (77.3 vs 75%, $p > 0.05$) (Fig. 4c). These results provide evidence of the biological significance of NCC function for GS and, more importantly, of the blunted activity of NCC carrying the novel mutation in a manner that closely resembles that induced by thiazides.

Discussion

The NCC shares a highly conserved amino acid sequence with other members of the electro-neutral cation-coupled cotransporters family [12], which feature twelve transmembrane portions harboring a central hydrophobic domain and two NH_2- and COOH-cytosolic terminal ends [13–15]. The central region, particularly the 7th and 8th domains, consists of the external loop with glycosylation sites and is held to be critical for ion translocation and binding of thiazides [7, 16].

The novel NCC c.1181G>A (G394D) mutation described here occurred in a heterozygous form in two young

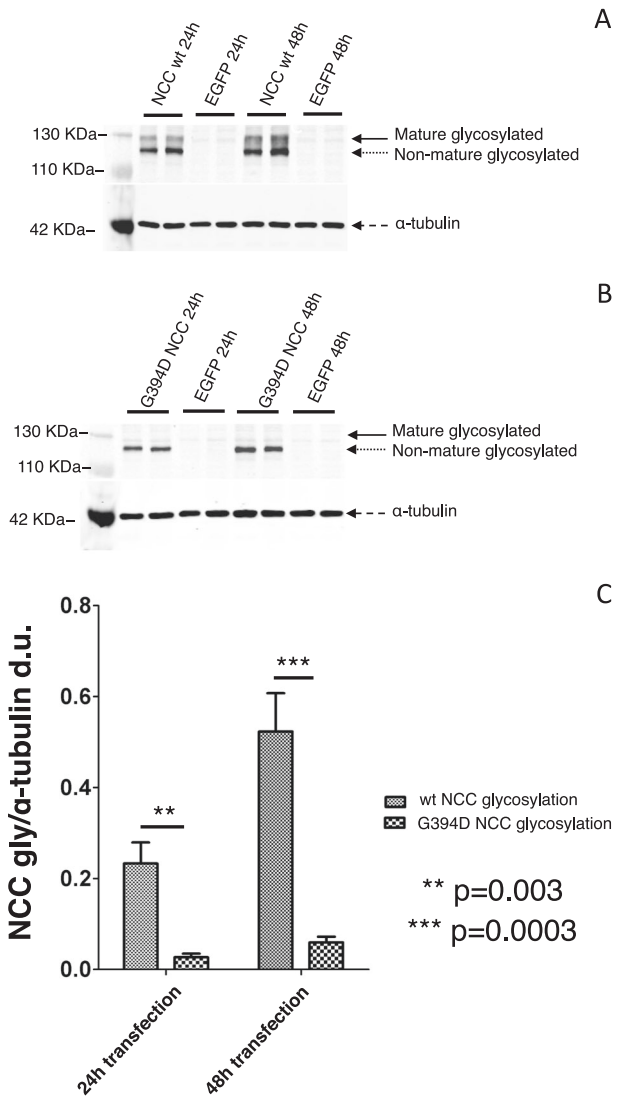

Fig. 3 **a** Immunoblots representative of HEK293 cells transfected with wt-NCC cDNA. Full and dotted arrows indicate the glycosylated and the non-glycosylated band, respectively. α-tubulin was used as housekeeping gene. **b** Immunoblots representative of HEK293 cells transfected with G394D-NCC cDNA. **c** Densitometric analysis of NCC glycosylation in wild-type and mutant cells 24 and 48 h after transfection

sisters with GS. However, a previously described concomitant mutation (c.1925G>A, R642H) [17] was also found by sequencing of 26 exons of SLC12A3 gene in both the index case and her sister, a finding consistent with the notion that concomitant mutations are often detected in GS patients [3, 12]. Whether an interaction between these concurrent mutations affects the protein activity and thereby the final GS phenotype has not been specifically addressed and remains to be clarified.

Over a decade ago, seminal studies with *X.L.* oocytes by Kunchaparty et al. and De Jong et al. opened the way to the functional characterization of NCC mutations underlying GS [18–27]. To date, based on functional and expression analyses in oocytes, five classes of NCC mutations in GS have been proposed (Table 1). In Class I, NCC mutants do not express NCC at the cell membrane, possibly because of loss of function caused by the lack of glycosylation and possibly other mechanisms leading to NCC retention inside the cells. In Class II, mutations alter the protein processing, causing its retention in the endoplasmic reticulum and degradation by enhanced endoplasmic reticulum-associated degradation (ERAD). NCC proteins in Class III mutations undergo glycosylation but are nonetheless poorly detectable on the cell membrane and unable to uptake Na^+, in contrast with Class IV mutants that can reach the membrane but exhibit strongly reduced Na^+ uptake. In Class V, mutations accelerate the protein removal from the plasma membrane and its degradation. In addition, some mutations are held to induce by exon skipping and synthesis of a non-functional protein, resulting, from the functional standpoint, in class III-like mutations [18, 19, 25, 28].

The novel mutation herein described is a missense single-nucleotide substitution of a glycine, a small neutral non-polar amino acid in position 394 of exon 9, with an aspartic acid residue, which carries a negative charge at physiological pH. This change influences the energy status and physical properties of the protein and thus its correct folding and function. Accordingly, our in vitro experiments showed a total loss of NCC function, thus unambiguously demonstrating the strong functional impact of this single amino acid change at this position. Importantly, $^{22}Na^+$ uptake experiments showed that the G394D mutation can account for GS: *X.L.* oocytes transfected with the mutant could uptake only 23% of the $^{22}Na^+$ when incubated in K^+-free medium compared to the wt-transfected NCC-transfected cells. Moreover, by blocking the activity of wt-NCC (to the level seen with vehicle injection), the thiazide metolazone left the basal $^{22}Na^+$ uptake in G394D-NCC unaffected, thus confirming that G394D-NCC either did not reach the plasma membrane or was not functional. Our immunofluorescence experiments support the first contention by showing intracellular retention of the mutated NCC protein (Fig. 4b).

Previous studies by Hoover et al. showed that the rat NCC has asparagine 404 and 424 N-linked sites that are critical for the glycosylation of the cotransporter [29, 30]. These glycosylation sites in the external loop are held to be key for the maturation of the protein and for the selectivity filter function; therefore, mutations in these positions predict loss of protein activity [16, 29]. Notably, these sites are located in the 7th trans-membrane fragment near the location of our novel mutation. We could show that both a human kidney cell line and X.L. oocytes transfected with the wt-NCC construct consistently showed two bands by immunoblotting, while mutant-

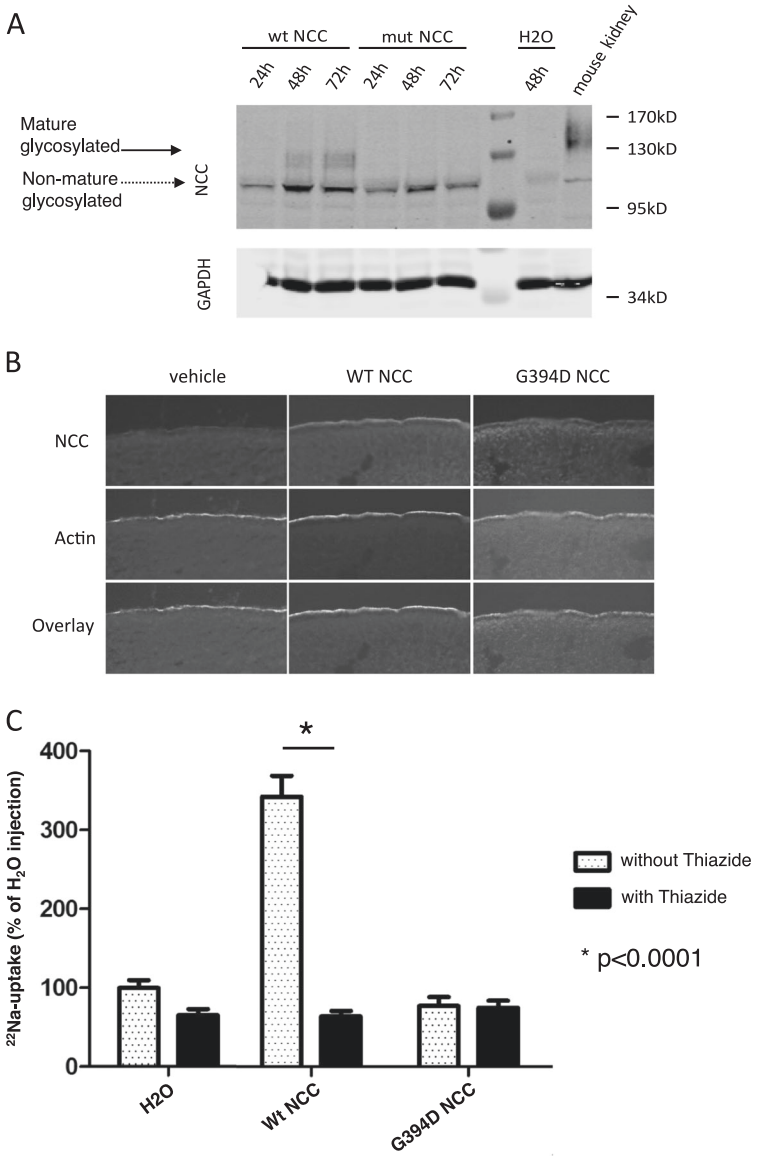

Fig. 4 **a** Western blot image of oocyte lysates analyzed with an antibody against NCC. A glycosylation band of approximately 130 KDa is expressed in wt-NCC cells but absent in mutant cells. GADPDH immunoreactivity serves as a loading control. **b** Immunohistochemical analyses of oocytes injected with 0.05 µl H_2O, wt-NCC, or G394D-NCC cRNA, respectively. Co-labeling with both antibodies against NCC and actin. Actin cytoskeleton is used as a housekeeping marker and shows membranous staining. wt-NCC immunostaining co-localizes with actin at the membrane, whereas G394D-NCC shows cytoplasmic immunostaining under the membrane. **c** $^{22}Na^{+}$ Uptake in oocytes injected and treated or not with thiazides. Control group H_2O: without thiazide 100 vs. with thiazide 65.01, $p > 0.05$; wt-NCC: without thiazide 342.3 vs. with thiazide 63.3, $p < 0.0001$; G394D-NCC: without thiazide 77.3 vs. with thiazide 75, $p > 0.05$

transfected cells did not show the higher-molecular weight band, suggesting the lack of the glycosylated form of the protein. However, additional mechanisms need to be considered. To prevent the expression of altered proteins, cells utilize complex mechanisms, such as the recruitment of chaperone molecules that lead to the denaturation of misfolded proteins [31]. With regard to GS, Needham et al. documented a blunted NCC export from the endoplasmic reticulum due to misfolding and an ERAD degradation [32]. Hence, we would like to propose that our novel misfolded NCC mutant follows a similar path and undergoes premature degradation by the ERAD system.

Overall, the present results with the G394D-NCC mutation, such as the lack of $^{22}Na^{+}$ uptake, the lack of a response to thiazides, the lack of a glycosylation band, and absence of detection on the plasma membrane, indicate that the G394D-NCC is retained in the ER, where it undergoes ERAD and therefore never reaches the plasma membrane, its functional site.

We took advantage of the novel mutation identified to assemble a summary of all known NCC mutations associated with GS by functional class in a single diagram depicting its channel structure. A closer look at the distribution of these mutations along the NCC structure (Fig. 2) clearly shows that no specific domain of the channel can be linked to any particular class of NCC mutations.

One more intriguing finding in this pedigree deserves comment: as repeatedly reported for GS [3, 7, 11], both the index case and her sister showed a concurrent GS NCC mutation. To gather insight as to why these differences occurred between sisters with the same mutations, we had

Table 1 Functional classification of NCC mutations identified in Gitelman's syndrome

Class nr. homozygotes	Exon	AA substitution	Domain	Ref.	Glycosylation	Detection on cell membrane	Na^+ uptake	Allele frequency
CLASS I: NCC mutants not exposed to the membrane								
0	4	S188F	2 TM	21	No	No	No	8.262e-06
0	10	G439S	6 TM	19	No	No	No	2.33e-04
na	16	T649R	CTD	19	No	No	No	na
0	18	G741R	CTD	19	No	No	No	3.97e-04
na	25	R968X	CTD	18	No	No	No	na
na	26	R1018X	CTD	18	No	No	No	na
Class II: NCC mutants causing ritention of peptide in ER and degradation by ERAD								
na	1	N59I	NTD	22	No	Cytoplasmic	No	na
0	1	T60M	NTD	23	No	Cytoplasmic	No	7.418e-05
0	1	R83W	NTD	22	No	Cytoplasmic	No	3.307e-05
na	5	R209W	IL	18	No	Cytoplasmic	No	1.21e-05
0	5	L215P	IL	19	No	Cytoplasmic	No	8.24e-06
0	7	T304M	5 TM	23	No	Cytoplasmic	No	8.24e-06
0	7	G316V	EL	24	No	Cytoplasmic	No	1.65e-05
na	8	P349L	6 TM	18	No	Cytoplasmic	No	4.06e-06
na	8	I360T	IL	22	No	Cytoplasmic	No	na
0	9	G394D	7TM	*this study*	No	Cytoplasmic	No	1.439e-05
0	10	C421Y	EL	22	No	Cytoplasmic	No	8.47e-06
0	10	C421R	EL	18	No	Cytoplasmic	No	8.47e-06
0	11	G463R	8 TM	22	No	Cytoplasmic	No	3.31e-05
na	11	T465P	8 TM	23	No	Cytoplasmic	No	na
0	13	F536L	10 TM	19	No	Cytoplasmic	No	8.23e-06
0	18	G731R	CTD	22	No	Cytoplasmic	No	2.48e-05
na	18	L738R	CTD	18	No	Cytoplasmic	No	na
0	22	L859P	CTD	22	No	Cytoplasmic	No	1.03e-04
0	22	R861C	CTD	22	No	Cytoplasmic	No	1.28e-04
na	24	R955Q	CTD	19	No	Cytoplasmic	No	na
na	25	G980R	CTD	19	No	Cytoplasmic	No	na
na	26	C985Y	CTD	19	No	Cytoplasmic	No	na
Class III: albeit glycosylated, NCC mutants barely detectable on the cell membrane and have impaired Na^+ uptake								
na	14	A585V	12 TM	20	Slight	Slight	Reduced	na
na	15	G610S	CTD	20	Slight	Slight	Reduced	na
na	15	N611T	CTD	23	Slight	Slight	Reduced	na
na	15	G627V	CTD	20	Slight	Slight	Reduced	na
na	24	R935Q	CTD	20	Slight	Slight	Reduced	na
na	26	V995M	CTD	20	Slight	Slight	Reduced	na
na	26	Q1030R	CTD	25	Slight	Slight	Reduced	8.23e-06
Exon	8	A356V	6 TM	28	Yes/No	Yes	No	na
skipping	16	M672I	CTD	28	Yes/No	Yes	No	na
Class IV: NCC mutants detectable on cell membrane but show markedly impaired Na^+ uptake								
1	2	E121D	NTD	25	Yes	Yes	Both	1.09e-03
0	3	R145C	1TM	26	Yes	Yes	Both	8.72e-06
na	10	N442S	EL	25	Yes	Yes	Both	na
na	12	Y489H	IL	25	Yes	Yes	Both	na
0	14	S555L	IL	27	Yes	Yes	Both	4.94e-05

Table 1 (continued)

Class nr. homozygotes	Exon	AA substitution	Domain	Ref.	Glycosylation	Detection on cell membrane	Na^+ uptake	Allele frequency
0	14	A588V	12 TM	27	Yes	Yes	Both	4.12e-05
0	18	P751L	IL	25	Yes	Yes	Both	9.12e-05
Class V: NCC mutants result into accelerated protein removal from cell membrane, ubiquitination, and/or degradation								
na	3	L155F	1 TM	21	Yes	Yes	Reduced	8.14e-06
na	5	A232T	3 TM	21	Yes	Yes	Reduced	1.2e-03
na	12	F495L	IL	21	Yes	Yes	Reduced	na
na	19	G779E	CTD	21	Yes	Yes	Reduced	4.06e-06

The mutants are functionally characterized with their location on the exon, their topological domain and their allele frequencies

TM transmembrane domain, *CTD* C-terminal domain, *NTD* N-terminal domain, *EL* extracellular loop, *IL* intracellular loop, *Both* both apical/cytoplasmic detection, *na* not available

the opportunity to follow them during pregnancy. Both sisters required additional K^+ and Mg^{2+} supplementation in order to maintain normal serum levels of the electrolytes, consistent with the literature [33]. However, after pregnancy, the individual needs of each sister returned to exactly the same levels as before pregnancy. Therefore, not even the physiological assessment during a stressful condition such as pregnancy provided any clues to explain the differences in severity of the clinical phenotypes.

Differences in clinical manifestations between subjects of the same family carrying the same mutations can indeed have many causes: interaction between non-allelic genes that control for the same character and/or differences in penetrance and expressivity. According to several studies, the impact of GS mutations on protein expression, glycosylation, and phosphorylation would widely influence the severity of the phenotype and the time of clinical presentation [8, 20, 34, 35]. In addition, unknown genetic and environmental modifiers can also contribute to the severity or even the appearance of GS. Moreover, as mentioned above, the interactions between concomitant mutations in causing GS have never been investigated in depth, not even in kin. Indeed, compensatory mechanisms could occur in other segments of the nephron for the regulation of electrolyte transport, thus contributing to phenotype variability [36]. In this regard, we believe that further specific investigative efforts are necessary in the future. The current practice of analyzing mutations at the single-gene level and not the whole exome likely limits the likelihood of determining whether and how other gene mutations could be associated with the phenotype of the disease [37–41].

In conclusion, through the functional characterization of a novel mutation in NCC, this study further shed light on the clinical manifestation of the syndrome with regard to its genotype and on the mechanisms whereby mutations are associated with GS. Although our study provides an important additional insight into this field, further studies are needed to provide correlations between genotype and phenotype.

Acknowledgements We thank Johannes Loffing's team of the Institute of Anatomy at UZH for their excellent technical and formative support. We also thank Prof. Zanotti, University of Padua, for kindly providing us the 3D structure of the mutated NCC protein.

Compliance with ethical standards

Conflict of interest The authors declare that they have no conflict of interest.

References

1. Blanchard A, Bockenhauer D, Bolignano D, Calo LA, Cosyns E, Devuyst O, Ellison DH, Karet Frankl FE, Knoers NV, Konrad M, Lin SH, Vargas-Poussou R. Gitelman syndrome: consensus and guidance from a Kidney Disease: Improving Global Outcomes (KDIGO) Controversies Conference. Kidney Int. 2017;91:24–33.
2. Gitelman HJ, Graham JB, Welt LG. A new familial disorder characterized by hypokalemia and hypomagnesemia. Trans Assoc Am Physicians. 1966;79:221–35.
3. Calo LA, Davis PA, Rossi GP. Understanding the mechanisms of angiotensin II signaling involved in hypertension and its long-term sequelae: Insights from Bartter's and Gitelman's syndromes, human models of endogenous angiotensin II signaling antagonism. J Hypertens. 2014;32:2109–19.
4. Ravarotto V, Pagnin E, Fragasso A, Maiolino G, Calò LA. Angiotensin II and cardiovascular-renal remodelling in hypertension: insights from a human model opposite to hypertension. High Blood Press Cardiovasc Prev. 2015;22:215–23.
5. Loffing J, Vallon V, Loffing-Cueni D, Aregger F, Richter K, Pietri L, Bloch-Faure M, Hoenderop JG, Shull GE, Meneton P, Kaissling B. Altered renal distal tubule structure and renal Na(+) and Ca(2+) handling in a mouse model for gitelman's syndrome. J Am Soc Nephrol. 2004;15:2276–88.
6. Ji W, Foo JN, O'Roak BJ, Zhao H, Larson MG, Simon DB, Newton-Cheh C, State MW, Levy D, Lifton RP. Rare independent mutations in renal salt handling genes contribute to blood pressure variation. Nat Genet. 2008;40:592–9.

7. Vargas-Poussou R, Dahan K, Kahila D, Venisse A, Riveira-Munoz E, Debaix H, Grisart B, Bridoux F, Unwin R, Moulin B, Haymann JP, Vantyghem MC, Rigothier C, Dussol B, Godin M, Nivet H, Dubourg L, Tack I, Gimenez-Roqueplo AP, Houillier P, Blanchard A, Devuyst O, Jeunemaitre X. Spectrum of mutations in Gitelman syndrome. J Am Soc Nephrol. 2011;22:693–703.
8. Wang L, Dong C, Xi YG, Su X. Thiazide-sensitive Na+ -Cl- cotransporter: genetic polymorphisms and human diseases. Acta Biochim Biophys Sin. 2015;47:325–34.
9. Mastroberardino L, Spindler B, Forster I, Loffing J, Assandri R, May A, Verrey F. Ras pathway activates epithelial Na+ channel and decreases its surface expression in Xenopus oocytes. Mol Biol Cell. 1998;9:3417–27.
10. Monroy A, Plata C, Hebert SC, Gamba G. Characterization of the thiazide-sensitive Na(+)-Cl(-) cotransporter: a new model for ions and diuretics interaction. Am J Physiol Ren Physiol. 2000;279: F161–9.
11. Knoers NV, Levtchenko EN. Gitelman syndrome. Orphanet J Rare Dis. 2008;3:22–1172-3-22.
12. Hediger MA, Romero MF, Peng JB, Rolfs A, Takanaga H, Bruford EA. The ABCs of solute carriers: physiological, pathological and therapeutic implications of human membrane transport proteins Introduction. Pflug Arch. 2004;447:465–8.
13. Gamba G. Molecular physiology and pathophysiology of electroneutral cation-chloride cotransporters. Physiol Rev. 2005;85:423–93.
14. Hebert SC, Mount DB, Gamba G. Molecular physiology of cation-coupled Cl- cotransport: the SLC12 family. Pflug Arch. 2004;447:580–93.
15. Hartmann AM, Tesch D, Nothwang HG, Bininda-Emonds OR. Evolution of the cation chloride cotransporter family: ancient origins, gene losses, and subfunctionalization through duplication. Mol Biol Evol. 2014;31:434–47.
16. Moreno E, Cristobal PS, Rivera M, Vazquez N, Bobadilla NA, Gamba G. Affinity-defining domains in the Na-Cl cotransporter: a different location for Cl- and thiazide binding. J Biol Chem. 2006;281:17266–75.
17. Colussi G, Bettinelli A, Tedeschi S, De Ferrari ME, Syren ML, Borsa N, Mattiello C, Casari G, Bianchetti MG. A thiazide test for the diagnosis of renal tubular hypokalemic disorders. Clin J Am Soc Nephrol. 2007;2:454–60.
18. Kunchaparty S, Palcso M, Berkman J, Velazquez H, Desir GV, Bernstein P, Reilly RF, Ellison DH. Defective processing and expression of thiazide-sensitive Na-Cl cotransporter as a cause of Gitelman's syndrome. Am J Physiol. 1999;277:F643–9.
19. De Jong JC, Van Der Vliet WA, Van Den Heuvel LP, Willems PH, Knoers NV, Bindels RJ. Functional expression of mutations in the human NaCl cotransporter: evidence for impaired routing mechanisms in Gitelman's syndrome. J Am Soc Nephrol. 2002;13:1442–8.
20. Sabath E, Meade P, Berkman J, de los Heros P, Moreno E, Bobadilla NA, Vázquez N, Ellison DH, Gamba G. Pathophysiology of functional mutations of the thiazide-sensitive Na-Cl cotransporter in Gitelman disease. Am J Physiol Ren Physiol. 2004;287:F195–203.
21. Acuna R, Martinez-de-la-Maza L, Ponce-Coria J, Vazquez N, Ortal-Vite P, Pacheco-Alvarez D, Bobadilla NA, Gamba G. Rare mutations in SLC12A1 and SLC12A3 protect against hypertension by reducing the activity of renal salt cotransporters. J Hypertens. 2011;29:475–83.
22. Valdez-Flores MA, Vargas-Poussou R, Verkaart S, Tutakhel OA, Valdez-Ortiz A, Blanchard A, Treard C, Hoenderop JG, Bindels RJ, Jelen S. Functionomics of NCC mutations in Gitelman syndrome using a novel mammalian cell-based activity assay. Am J Physiol Ren Physiol. 2016;311:F1159–67.
23. Miao Z, Gao Y, Bindels RJ, Yu W, Lang Y, Chen N, Ren H, Sun F, Li Y, Wang X, Shao L. Coexistence of normotensive primary aldosteronism in two patients with Gitelman's syndrome and novel thiazide-sensitive Na-Cl cotransporter mutations. Eur J Endocrinol. 2009;161:275–83.
24. Syren ML, Tedeschi S, Cesareo L, Bellantuono R, Colussi G, Procaccio M, Alì A, Domenici R, Malberti F, Sprocati M, Sacco M, Miglietti N, Edefonti A, Sereni F, Casari G, Coviello DA, Bettinelli A. Identification of fifteen novel mutations in the SLC12A3 gene encoding the Na-Cl Co-transporter in Italian patients with Gitelman syndrome. Hum Mutat. 2002;20:78.
25. Glaudemans B, Yntema HG, San-Cristobal P, Schoots J, Pfundt R, Kamsteeg EJ, Bindels RJ, Knoers NV, Hoenderop JG, Hoefsloot LH. Novel NCC mutants and functional analysis in a new cohort of patients with Gitelman syndrome. Eur J Hum Genet. 2012;20:263–70.
26. Riveira-Munoz E, Chang Q, Godefroid N, Hoenderop JG, Bindels RJ, Dahan K, Devuyst O. Belgian Network for Study of Gitelman Syndrome. Transcriptional and functional analyses of SLC12A3 mutations: new clues for the pathogenesis of Gitelman syndrome. J Am Soc Nephrol. 2007;18:1271–83.
27. Simon DB, Nelson-Williams C, Bia MJ, Ellison D, Karet FE, Molina AM, Vaara I, Iwata F, Cushner HM, Koolen M, Gainza FJ, Gitelman HJ, Lifton RP. Gitelman's variant of Bartter's syndrome, inherited hypokalaemic alkalosis, is caused by mutations in the thiazide-sensitive Na-Cl cotransporter. Nat Genet. 1996;12:24–30.
28. Takeuchi Y, Mishima E, Shima H, Akiyama Y, Suzuki C, Suzuki T, Nakayama T, Takeshima Y, Vazquez N, Ito S, Gamba G, Abe T. Exonic mutations in the SLC12A3 gene cause exon skipping and premature termination in Gitelman syndrome. J Am Soc Nephrol. 2015;26:271–9.
29. Hoover RS, Poch E, Monroy A, Vazquez N, Nishio T, Gamba G, Hebert SC. N-Glycosylation at two sites critically alters thiazide binding and activity of the rat thiazide-sensitive Na(+):Cl(-) cotransporter. J Am Soc Nephrol. 2003;14:271–82.
30. De Jong JC, Willems PH, Mooren FJ, van den Heuvel LP, Knoers NV, Bindels RJ. The structural unit of the thiazide-sensitive NaCl cotransporter is a homodimer. J Biol Chem. 2003;278:24302–7.
31. Wang M, Kaufman RJ. Protein misfolding in the endoplasmic reticulum as a conduit to human disease. Nature. 2016;529:326–35.
32. Needham PG, Mikoluk K, Dhakarwal P, Khadem S, Snyder AC, Subramanya AR, Brodsky JL. The thiazide-sensitive NaCl cotransporter is targeted for chaperone-dependent endoplasmic reticulum-associated degradation. J Biol Chem. 2011;286:43611–21.
33. Calò LA, Caielli P. Gitelman's syndrome and pregnancy: new potential pathophysiological influencing factors, therapeutic approach and materno-fetal outcome. J Matern Fetal Neonatal Med. 2012;25:1511–3.
34. Riveira-Munoz E, Chang Q, Bindels RJ, Devuyst O. Gitelman's syndrome: towards genoype-phenotype correlations? Pediatr Nephrol. 2007;22:326–32.
35. Tseng MH, Yang SS, Hsu YJ, Fang YW, Wu CJ, Tsai JD, Hwang DY, Lin SH. Genotype, phenotype, and follow-up in Taiwanese patients with salt-losing tubulopathy associated with SLC12A3 mutation. J Clin Endocrinol Metab. 2012;97:E1478–82.
36. Loffing J, Loffing-Cueni D, Valderrabano V, Kläusli L, Hebert SC, Rossier BC, Hoenderop JG, Bindels RJ, Kaissling B. Distribution of transcellular calcium and sodium transport pathways along mouse distal nephron. Am J Physiol Ren Physiol. 2001;281:1021.
37. Lin SH, Cheng NL, Hsu YJ, Halperin ML. Intrafamilial phenotype variability in patients with Gitelman syndrome having the

same mutations in their thiazide-sensitive sodium/chloride cotransporter. Am J Kidney Dis. 2004;43:304–12.
38. Lin SH, Shiang JC, Huang CC, Yang SS, Hsu YJ, Cheng CJ. Phenotype and genotype analysis in Chinese patients with Gitelman's syndrome. J Clin Endocrinol Metab. 2005;90:2500–7.
39. Delpire E, Mount DB. Human and murine phenotypes associated with defects in cation-chloride cotransport. Annu Rev Physiol. 2002;64:803–43.
40. Balavoine AS, Bataille P, Vanhille P, Azar R, Noel C, Asseman P, Soudan B, Wémeau JL, Vantyghem MC. Phenotype-genotype correlation and follow-up in adult patients with hypokalaemia of renal origin suggesting Gitelman syndrome. Eur J Endocrinol. 2011;165:665–73.
41. Al Shibli A,Narchi H, Bartter and Gitelman syndromes: spectrum of clinical manifestations caused by different mutations. World J Methodol. 2015;5:55–61.